AD-A080 953 DAVID W TAYLOR NAVAL SHIP RESEARCH AND DEVELOPMENT CE--ETC F/G 20/4
THE EFFECT OF SHAFT ANGLE ON PERFORMANCE OF A CIRCULATION CONTR--ETC(U)
FEB 80 K R READER

UNCLASSIFIED AERO-1262 DTNSRDC-80/015 NL

1 OF 1
AD-
A080953

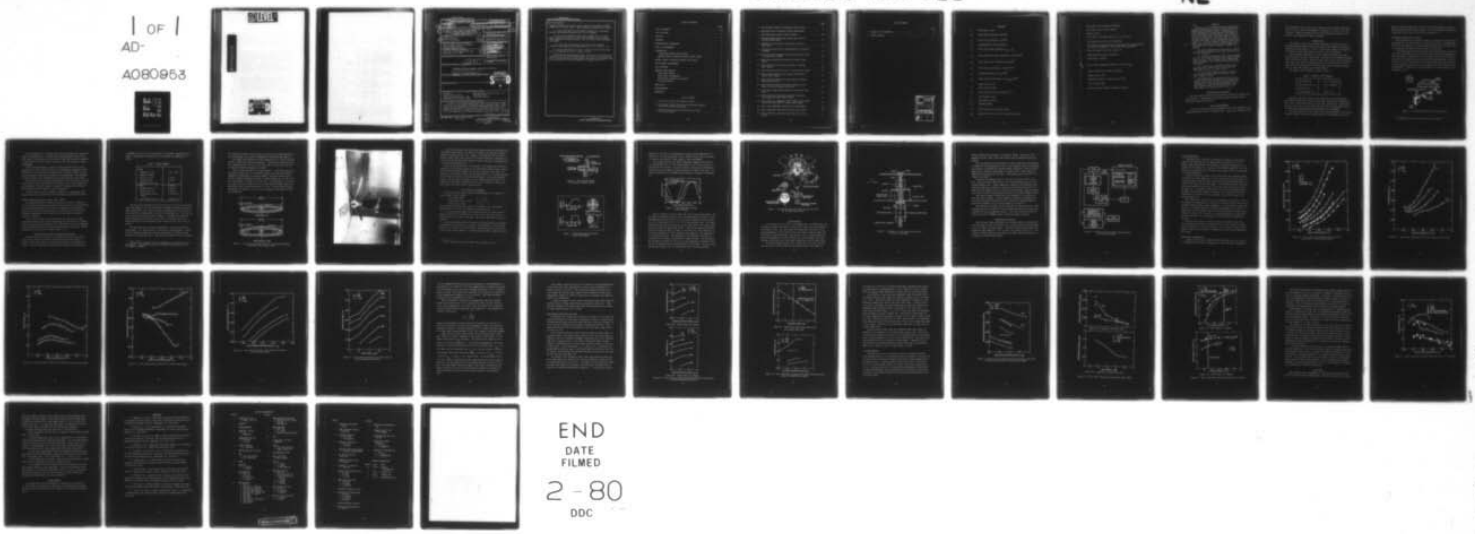

END
DATE
FILMED
2-80
DDC

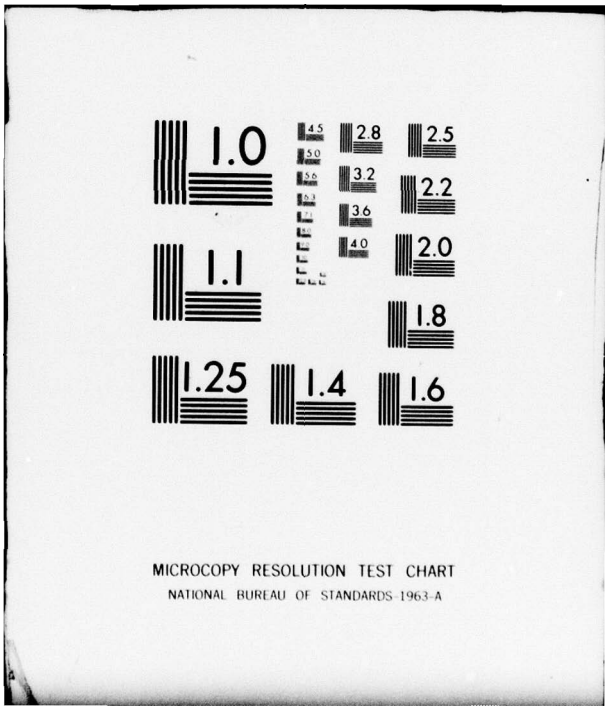
1.0
1.1
1.25
1.4
1.6
1.8
2.0
2.2
2.5
2.8
3.2
3.6
4.0
4.5
5.0
5.6
6.3
MICROCOPY RESOLUTION TEST CHART
NATIONAL BUREAU OF STANDARDS-1963-A

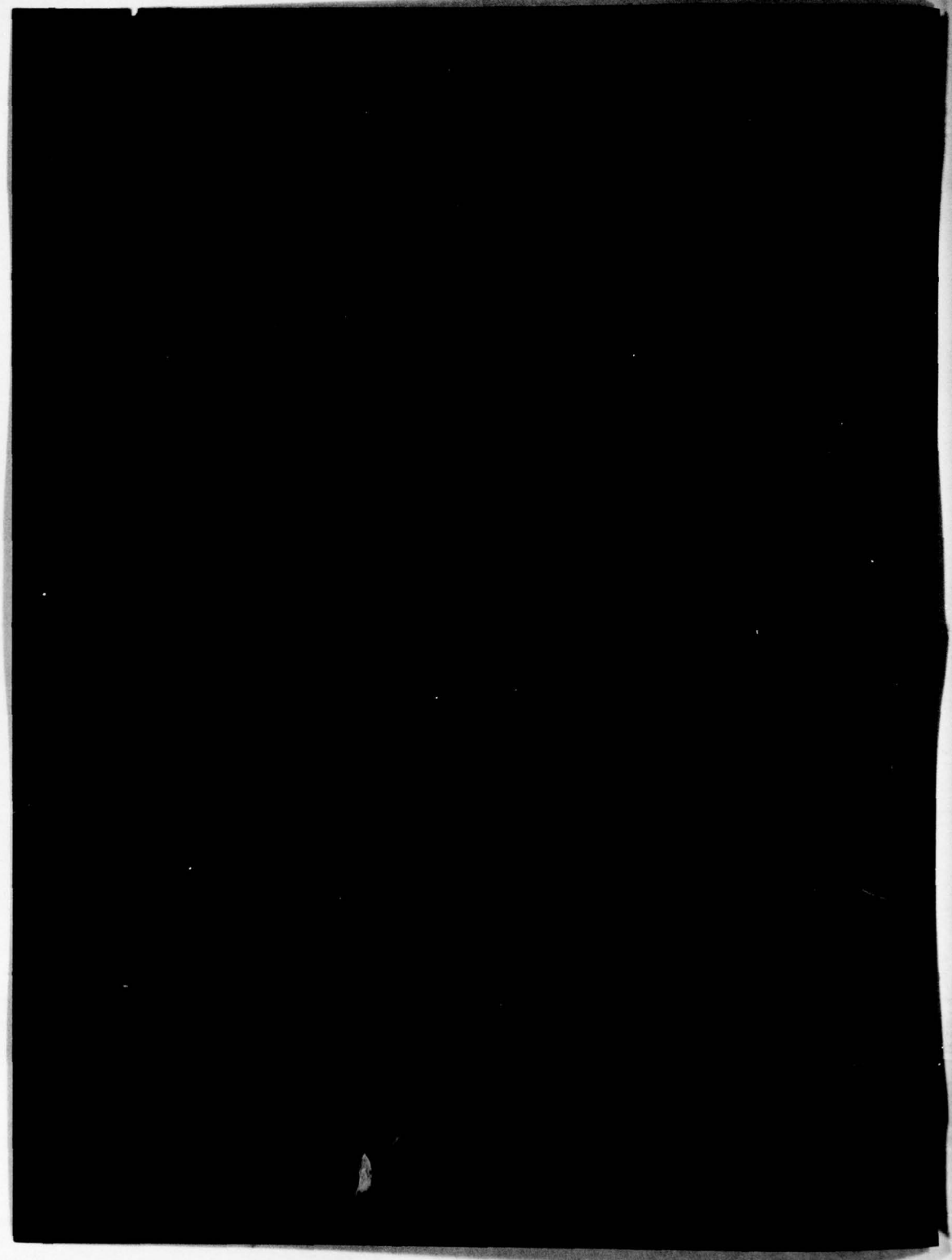

UNCLASSIFIED

SECURITY CLASSIFICATION OF THIS PAGE (When Data Entered)

(19) REPORT DOCUMENTATION PAGE

READ INSTRUCTIONS BEFORE COMPLETING FORM

(18) 1. REPORT NUMBER: DTNSRDC-80/015

2. GOVT ACCESSION NO. (9) Research and development

3. RECIPIENT'S CATALOG NUMBER

(6) 4. TITLE (and Subtitle): THE EFFECT OF SHAFT ANGLE ON PERFORMANCE OF A CIRCULATION CONTROL HIGH-SPEED ROTOR AT AN ADVANCE RATIO OF 0.7

5. TYPE OF REPORT & PERIOD COVERED: Formal rept.

6. PERFORMING ORG. REPORT NUMBER: Aero Report 1262

(10) 7. AUTHOR(s): Kenneth R. Reader

(14) 8. CONTRACT OR GRANT NUMBER(s): AERO-1262

9. PERFORMING ORGANIZATION NAME AND ADDRESS
David W. Taylor Naval Ship Research and Development Center
Bethesda, Maryland 20084

(17) 10. PROGRAM ELEMENT, PROJECT, TASK AREA & WORK UNIT NUMBERS
Element 62543N
Proj WF41 421 210
Work [redacted]

(11) 11. CONTROLLING OFFICE NAME AND ADDRESS
Naval Air Systems Command (AIR 320D)
Washington, D.C. 20361

12. REPORT DATE
Feb [redacted] 80

13. NUMBER OF PAGES
40

14. MONITORING AGENCY NAME & ADDRESS(if different from Controlling Office)

(12) 45

15. SECURITY CLASS. (of this report)
UNCLASSIFIED

15a. DECLASSIFICATION/DOWNGRADING SCHEDULE

16. DISTRIBUTION STATEMENT (of this Report)

APPROVED FOR PUBLIC RELEASE: DISTRIBUTION UNLIMITED

(16) F41421

17. DISTRIBUTION STATEMENT (of the abstract entered in Block 20, if different from Report)

DTIC ELECTE FEB 21 1980 S D B

18. SUPPLEMENTARY NOTES

19. KEY WORDS (Continue on reverse side if necessary and identify by block number)

Helicopter
Boundary Layer Control
Circulation Control Rotor (CCR)
High-Speed Rotor--Forward Flight
High-Speed Rotor--Advance Ratio = 0.7
Tip Speed Effects
Shaft Angle Effects

20. ABSTRACT (Continue on reverse side if necessary and identify by block number)

As part of the on-going Circulation Control Rotor Technology Program at the David W. Taylor Naval Ship Research and Development Center, a high-speed rotor model designated the Reverse Blowing Circulation Control Rotor (RBCCR) was evaluated in a wind tunnel in the forward flight mode. The RBCCR model was used to evaluate the effects of rotor shaft angle of attack on rotor performance at the transitional advance ratio of $\mu = 0.7$. The test

(Continued on reverse side)

DD FORM 1 JAN 73 1473 EDITION OF 1 NOV 65 IS OBSOLETE
S/N 0102-014-6601

UNCLASSIFIED

SECURITY CLASSIFICATION OF THIS PAGE (When Data Entered)

387695

(Block 20 continued)

variables included rotor thrust, blade collective pitch angle, tip Mach number, and rotor shaft angle. Major findings are summarized as follows:

(1) Rotor performance has been shown to improve by a substantial amount as shaft angle increases from -5 to +2.5 degrees.

(2) The rotor experiences better thrust augmentation at a fixed blade collective pitch angle as shaft angle increases. The increased thrust augmentation results in better rotor efficiencies with increasing shaft angle.

(3) A trim limit relationship between shaft angle and blade collective pitch angle has been established to be $\theta_c = -0.6647\ \alpha_s - 0.7$.

(4) As the shaft angle is varied, a trade-off exists between shaft power and compressor power over a range of thrust.

The RBCCR model has demonstrated both the lift and trim capabilities required in the transitional flight regime. The model has also shown that rotor efficiency and power sharing between shaft power and compressor power can be controlled by rotor shaft angle at an advance ratio of 0.7.

TABLE OF CONTENTS

LIST OF FIGURES

LIST OF TABLES

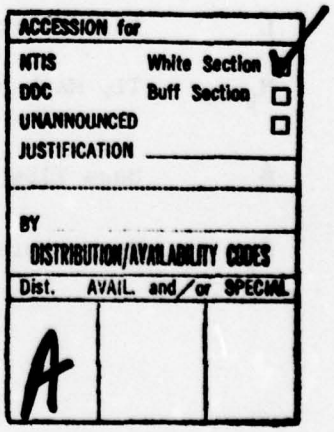

NOTATION

b	Blade span in feet
C_D	Rotor drag coefficient, $D/\rho\pi\Omega^2R^4$
C_L	Rotor lift coefficient, $L/\rho\pi\Omega^2R^4$
C_ℓ	Two-dimensional lift coefficient
C_p	Rotor total power coefficient, $C_{p_s} + C_{p_c}$
C_{p_c}	Rotor compressor power coefficient, $\dot{m} V_j^2/2\rho\pi\Omega^3R^5$
C_{p_s}	Rotor shaft power coefficient, $Q\Omega/\rho\pi\Omega^3R^5$
C_T	Rotor thrust coefficient, thrust$/\rho\pi\Omega^2R^4$
C_μ	Blowing coefficient, $\dot{m} V_j/\rho\pi\Omega^2R^4$
C_{μ_R}	Rotor blowing coefficient, $\dot{m}_T (V_j)_{max}/\rho\pi\Omega^2R^4$
c	Blade chord in feet
D	Rotor drag in pounds
D_e	Rotor equivalent drag in pounds, $\frac{P}{V} + D$
h	Slot height in feet
L	Rotor lift in pounds
M_T	Tip Mach number
$\dot{m}$	Mass flow rate in slugs per second
$\dot{m}_T$	Rotor total mass flow rate in slugs per second

P	Rotor shaft plus compressor horsepower
Q	Rotor shaft torque in foot pounds
R	Radius in feet
T	Rotor thrust in pounds, drag sin α_s + lift cos α_s
V	Free stream velocity in feet per second
V_j	Jet velocity in feet per second (calculated from the peak blade root pressure expanded to free stream static pressures)
V_T	Rotor tip speed in feet per second, ΩR
x	Dimensionless distance along radius
α_s	Shaft angle in degrees
$\frac{\Delta C_T}{\Delta C_{\mu_R}}$	Rotor thrust augmentation $\left(\text{slope of } C_T \text{ versus } C_{\mu_R}\right)$
θ_c	Blade collective pitch angle in degrees
μ	Advance ratio, $V/\Omega R$
ρ	Atmosphere density in slugs per cubic feet
σ	Rotor solidity, $\frac{4c}{\pi b}$
Ω	Rotor rotational speed in radians per second

ABSTRACT

As part of the on-going Circulation Control Rotor Technology Program at the David W. Taylor Naval Ship Research and Development Center, a high-speed rotor model designated the Reverse Blowing Circulation Control Rotor (RBCCR) was evaluated in a wind tunnel in the forward flight mode. The RBCCR model was used to evaluate the effects of rotor shaft angle of attack on rotor performance at the transitional advance ratio of $\mu = 0.7$. The test variables included rotor thrust, blade collective pitch angle, tip Mach number, and rotor shaft angle. Major findings are summarized as follows:

(1) Rotor performance has been shown to improve by a substantial amount as shaft angle increases from -5 to +2.5 degrees.

(2) The rotor experiences better thrust augmentation at a fixed blade collective pitch angle as shaft angle increases. The increased thrust augmentation results in better rotor efficiencies with increasing shaft angle.

(3) A trim limit relationship between shaft angle and blade collective pitch angle has been established to be $\theta_c = -0.6647\ \alpha_s - 0.7$.

(4) As the shaft angle is varied, a trade-off exists between shaft power and compressor power over a range of thrust.

The RBCCR model has demonstrated both the lift and trim capabilities required in the transitional flight regime. The model has also shown that rotor efficiency and power sharing between shaft power and compressor power can be controlled by rotor shaft angle at an advance ratio of 0.7.

ADMINISTRATIVE INFORMATION

The work reported herein was sponsored by the Naval Air Systems Command (AIR 320). Funding was provided under Element 62241N; Project F41.421.210; Work Unit 1619-111.

UNITS OF MEASUREMENTS

All data recorded during this experiment were either measured in (or converted directly to) U.S. customary units. Hence, U.S. customary units

are the primary units in this report. Metric units are given either adjacent to the U.S. units in parentheses or opposite U.S. units in the case of graphs. Angular measurement is the only exception and the unit of degrees is not converted to radians on graphs.

INTRODUCTION

The subject of this report is the evaluation of a 6.67-ft (2.03-m), high-speed Reverse Blowing Circulation Control Rotor (RBCCR) model in the transitional speed range ($\mu = 0.70$) at various shaft angles, to determine the effects of rotor shaft angle of attack on rotor performance.

Test variables included rotor thrust, blade collective pitch angle, tip Mach number, and rotor shaft angle. The major rotor parameters measured (total power, shaft power, compressor power, rotor thrust, rotor efficiency, rotor drag, mass flow rate, blade pressure, etc.) were plotted in coefficient form for constant blade collective pitch angle and constant advance ratio at fixed shaft angles and tip Mach number.

The range of test variables is given in Table 1.

TABLE 1 - RANGE OF TEST VARIABLES

Shaft Angle, α_s	-5 to 2.5 degrees
Blade Collective, θ_c	0 to -6 degrees
Advance Ratio, μ	0.7
Tip Mach Number, M_T	0.09 to 0.22

Because of the large volume of data obtained in these experiments, this report contains only the most significant findings and trade-offs for the rotor at shaft angles from +2.5 to -5 deg. The complete (unpublished) data set is on file in the Aviation and Surface Effects Department, David W. Taylor Naval Ship Research and Development Center (DTNSRDC).

The data presented in this report are directly applicable to the X-Wing aircraft; however, due to the extended range of the parameters above and

below the X-Wing design point, the data are also applicable to any high-speed Circulation Control Rotor concept. For a more detailed discussion of a high-speed rotor aircraft concept, see Reference 1.*

CIRCULATION CONTROL ROTOR CONCEPT

The application of Circulation Control (CC) airfoils to helicopters is predicated on: (1) their ability to increase the airfoil two-dimensional (2-D) lift coefficient (C_ℓ) at fixed angle of attack; and, (2) their ability to generate very high C_ℓ without angle of attach stall.

Circulation Control airfoils provide these characteristics by means of thin jets of compressed air, blown from slots within the trailing edges of the rotor blades. Specifically, the Circulation Control Rotor (CCR) concept involves a shaft-driven rotor with blades having circulation control airfoils. The CC airfoils employ a rounded trailing edge with a thin jet of air tangentially ejected from a slot adjacent to this (Coanda) surface (see Figure 1). Airfoil lift is proportional to the momentum flux of the exiting jet of air.

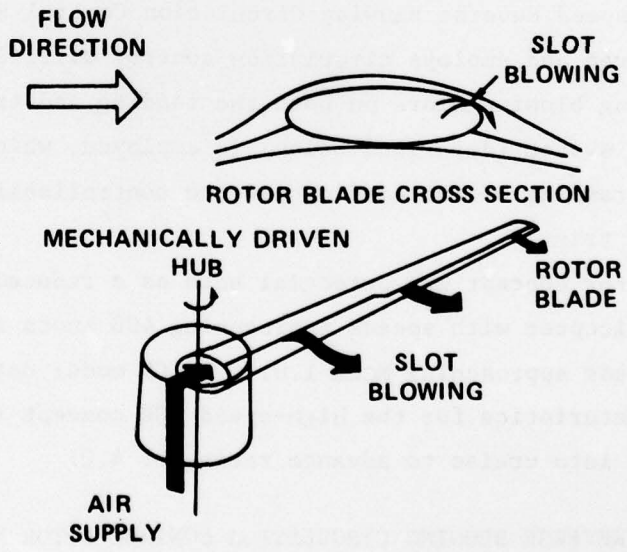

Figure 1 - Circulation Control Rotor--Basic Concept

*A complete listing of references is given on page 33.

The CCR requires an air supply duct within each blade and a continuous supply of compressed air. A simple throttling mechanism is used in the rotor head to provide control over both the cyclic and collective components of the blown air in order to meet the rotor cyclic and collective control requirements.

This process eliminates the need for blade mechanical cyclic pitch change and (in future evolutions) may also eliminate the mechanical collective pitch. The rotor head is therefore free of numerous dynamic control system components, which greatly simplifies the mechanisms. By presenting a cleaner profile, this configuration also reduces external rotor drag.

The CCR concept has been well-established in Navy and industry studies, and by extensive wind tunnel evaluation at model scale. These results and descriptions of the basic concept, as applied to helicopters operating in the conventional speed regime, are well-documented.[2-7]

The CCR concept has been extended at DTNSRDC to a high-speed, high advance ratio rotor system--the Reverse Blowing Circulation Control Rotor.

REVERSE BLOWING CIRCULATION CONTROL ROTOR CONCEPT

The high-speed Reverse Blowing Circulation Control Rotor (RBCCR) is also shaft-driven and employs circulation control airfoil sections modified by incorporating blowing slots on both the leading and trailing edges. A unique control system (described below) is employed, which enables both azimuthal programming of the airflow and the controllability needed to maintain rotor trim.

Such a rotor concept has potential both as a reduced-rpm, thrust-compounded helicopter with speeds approaching 400 knots and as a stoppable rotor with speeds approaching Mach 1.0.[8] RBCCR model data have established baseline characteristics for the high-speed CCR concept from hover through transition and into cruise to advance ratios of 4.0.

REVERSE BLOWING CIRCULATION CONTROL ROTOR MODEL

Previous analytical studies of the RBCCR concept have established a baseline rotor design in terms of operational thrust-coefficient-to-solidity ratio, blade twist, and airfoil distributions of thickness and camber. The resulting RBCCR configuration was designed and manufactured

at DTNSRDC as a 6.67-ft (2.03-m) diameter, four-bladed, untwisted rotor model.* The physical characteristics of the model are summarized in Table 2.

TABLE 2 - MODEL GEOMETRY

BLADE	
Diameter, ft (m)	6.67 (2.03)
Number of Blades	4
Chord, in. (cm)	5 (12.7)
Solidity Ratio	0.1592
Geometric Twist, deg	0
AIRFOIL	ROOT/TIP
Thickness Ratio, t/c	0.20/0.15
Camber Ratio, δ/c	0.05/0.0
Trailing Edge Radius, R_{TE}/c	0.052/0.022
Slot Height Ratio, h/c	0.002/0.002

The tests were conducted in the 8 by 10 ft (2.44 by 3.05 m) North Subsonic Wind Tunnel and on the hover stand of DTNSRDC's Aviation and Surface Effects Department. The airfoil sections were symmetrical about the mid-chord with both a leading edge slot and a trailing edge slot. The root and tip CC airfoil profiles are shown in Figure 2. Thickness distribution varied linearly from 20 percent at the root to 15 percent at the tip. Camber distribution varied linearly from 5 percent at the root to zero at the tip.

Slot positions were a constant percentage of chord over the entire blade length: x/c (leading edge) = 0.032 and x/c (trailing edge) = 0.968. The slot height-to-chord ratio was also constant (h/c = 0.002) for both leading and trailing edge slots. Each slot was supplied air from a separate

*This work was conducted under the sponsorship of the Naval Air Systems Command. The analytical study was performed, among others, by Mr. E.O. Rogers at DTNSRDC.

duct within the blade so that blowing from either the leading edge slot or the trailing edge slot could be independently controlled (see Figure 2).

The blades were machined from solid aluminum alloy in upper and lower halves by numerically controlled machines. Internal duct geometry and the slot regulating posts were cut at the same time to ensure equal mass and stiffness distributions between the blades.

Figure 3 shows the RBCCR in the wind tunnel. It should be noted that the model solidity ratio is considerably larger than that which would be designed or required for a full-scale RBCCR. The scaled chord for the correct solidity would have resulted in a model chord of 3.2 in. (8.13 cm) and a slot height of 0.0056 in. (0.0142 cm). The requirement of two slots per blade (and two air supply ducts per blade) made this small chord very impractical from a manufacturing point of view. The chord was therefore arbitrarily increased to 5 in. (12.7 cm), allowing a slot height of 0.010 in. (0.0254 cm).

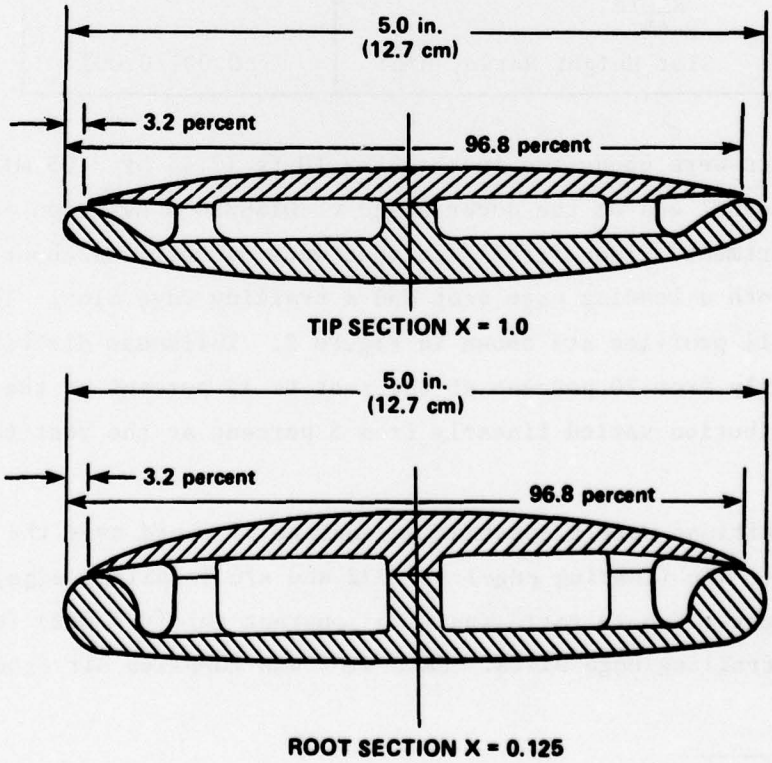

Figure 2 - Tip and Root Airfoil Sections of the Reverse Blowing Circulation Control Rotor Blade

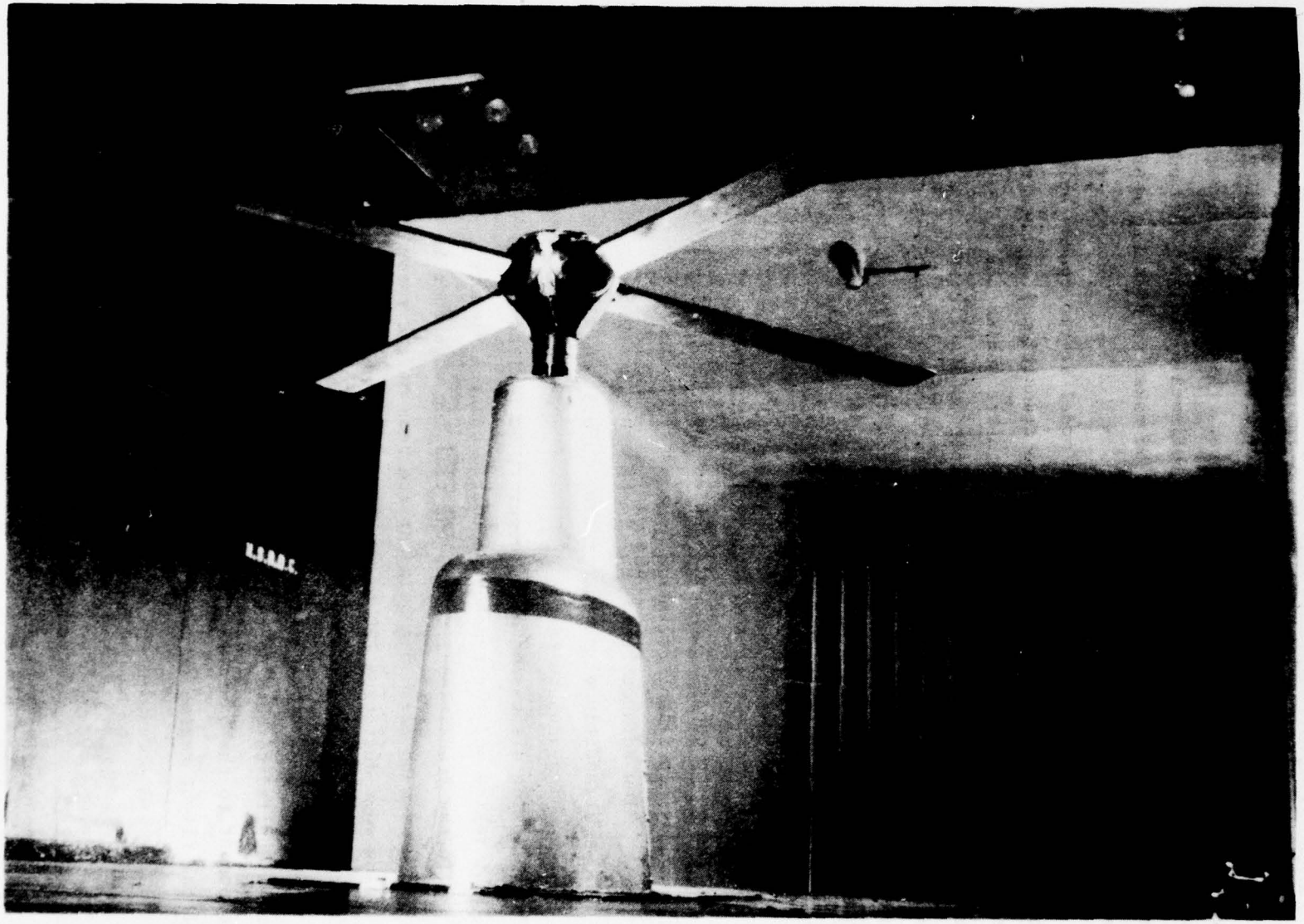

Figure 3 - Reverse Blowing Circulation Control Rotor Model in the Wind Tunnel

It was also realized that this would increase loads and therefore provide more accurate data at the reduced tip speeds corresponding to model operation at high advance ratio. However, this approach gave the model blades a lower aspect ratio than the full-scale design (8 as opposed to 10 to 12), so that the model data cannot be taken as directly representative of a full-scale high-speed rotor.

Also, it was necessary to run the model at tip speeds below those intended for the full-scale blades at the transitional advance ratio. While this did not scale Mach number, the data are scaled for C_T/σ, which accounts for the reduced tip speed and increased solidity. The data presented have not been corrected to full-scale Mach number or full-scale Reynolds number. All data points represent a fully trimmed condition (shaft roll moment and pitch moment trimmed to zero by cyclic control) at the thrust level (C_T/σ) indicated unless otherwise noted.

ROTOR CONTROL REQUIREMENTS

The basic control concept enables the RBCCR model to be trimmed in three distinct flight regimes:

low advance ratio	$0 < \mu < 0.5$,
transitional advance ratio	$0.5 \leq \mu \leq 1.4$,
high advance ratio	$\mu > 1.4$.

The following discussion will, however, be limited to the transitional flight regime and the type of pneumatic control required.

In the transitional range, the trailing edge duct is blown from 0 to 360 deg azimuth (zero deg being at the rear of the rotor disc) and the leading edge duct from 180 to 360 deg. This mode of operation is shown in Figure 4.

In the dual-blowing region of the disc (retreating side), the pressure waves applied to both ducts are the same. The addition of a 2P* pressure component to the basic 1P has been shown to be beneficial for this portion of the flight regime (Figure 5). Typical pressure control signals that are

*NP--occuring N time per revolution where N equals 1 or 2.

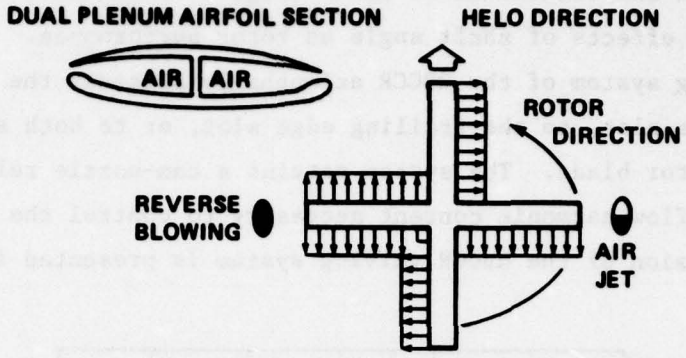

Figure 4 - Dual Blowing Concept
for Transition Advance Ratios

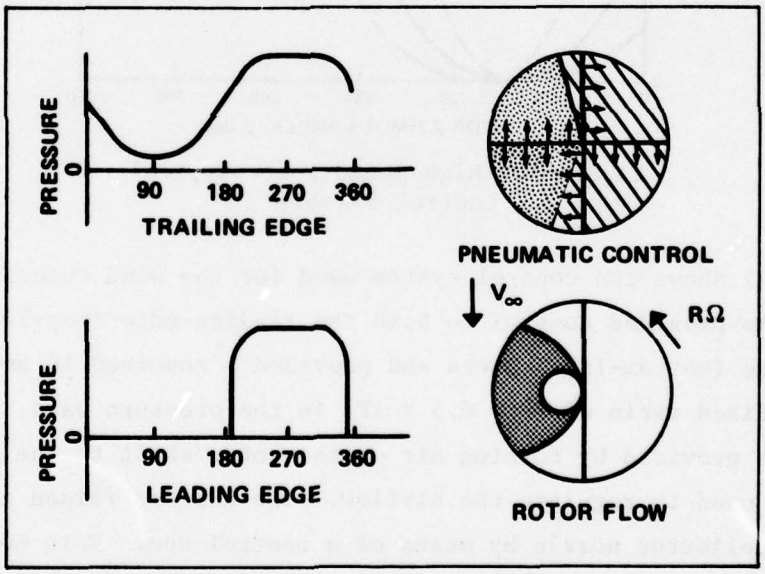

Figure 5 - High-Speed Rotor Transition
Control Requirements

produced by the cams of the RBCCR model can have various amounts of 2P (Figure 6). The cam identified as cam 2 (Figure 6) was used in the model to evaluate the effects of shaft angle on rotor performance.

The valving system of the RBCCR azimuthally programs the airflow to the leading edge slot, to the trailing edge slot, or to both slots of a dual-slotted rotor blade. The system retains a cam-nozzle relationship to provide the airflow harmonic content necessary to control the rotor. (A detailed discussion of the RBCCR valving system is presented in Reference 9.)

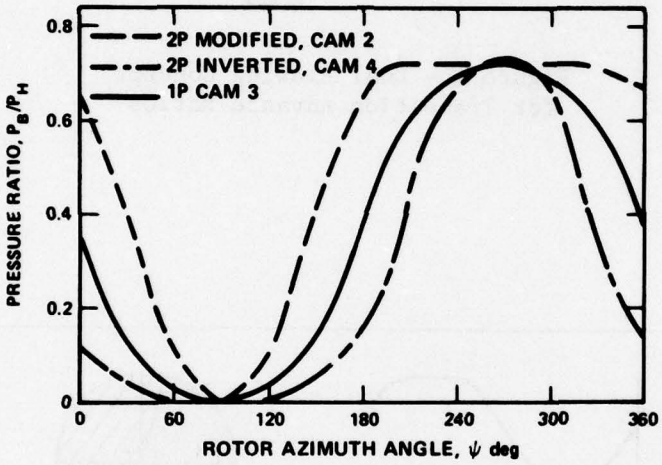

Figure 6 - High-Speed Rotor Typical Control Signals

Figure 7 shows the control system used for the wind tunnel model. The two-lobed cam provided control to both the leading-edge (top-lobe) and the trailing-edge (bottom-lobe) ducts and provided a combined 1P and 2P variation (at a fixed ratio of 2P = 0.5 × 1P) in the pressure wave. The control pressure was provided by forcing air up the rotor shaft to the head, where the cam was used to regulate the airflow. The cam was raised and lowered inside the collector nozzle by means of a control rod. This movement controlled the amplitude of cyclic pressure and, indirectly, the magnitude of the collective pressure. The magnitude of the collective was primarily controlled by the overall pressure level inside the head. Control phasing was achieved by turning the control rod, thus changing the azimuthal location of the maximum pressure being supplied to the blades. Once the proper setting was achieved, the only moving parts were the rotating blades.

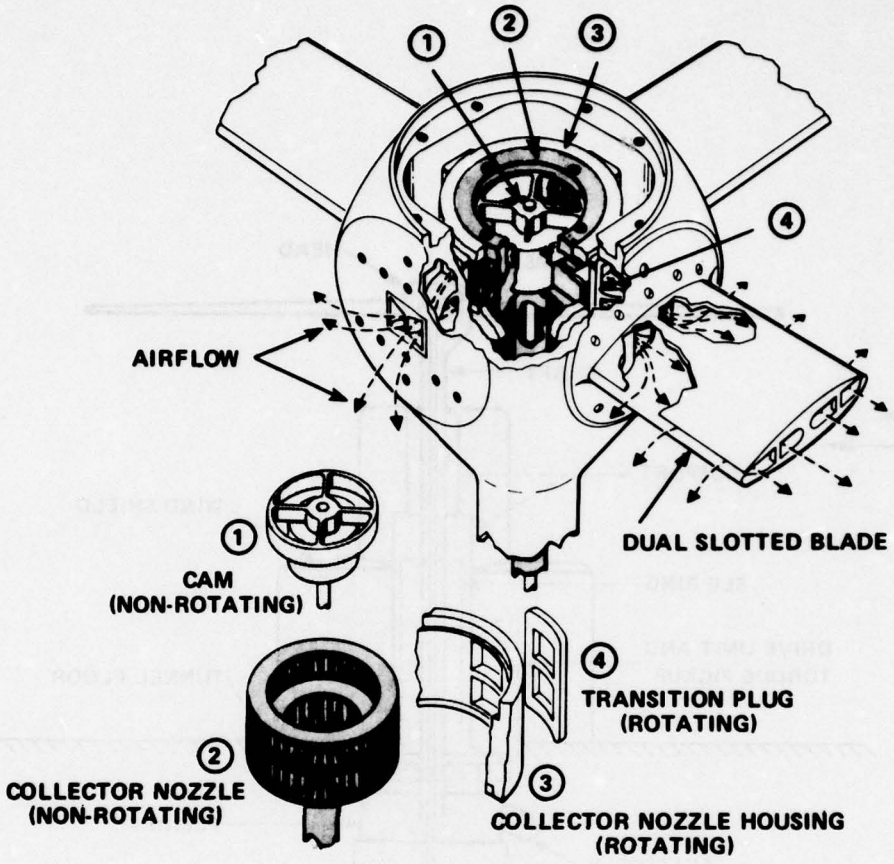

Figure 7 - Reverse Blowing Circulation Control Rotor Hub for the Wind Tunnel Model

TEST PROCEDURE

In the period 13 July 1976 to 17 September 1976, the RBCCR model was evaluated to assess the effects of rotor shaft angle on the performance of the isolated rotor. The rotor model was located with the center of the head approximately at the center of the test section, when the shaft was at 90 deg to freestream (shaft angle equal to zero). Figure 8 shows the general arrangement of the rotor system, with its 90-channel slip ring, hydraulic drive motor and torque meter, plenum box, and air supply line.

The tunnel balance measured lift, drag, pitch, roll, yaw, and side. The cam control rod went down into the tunnel control room, where the

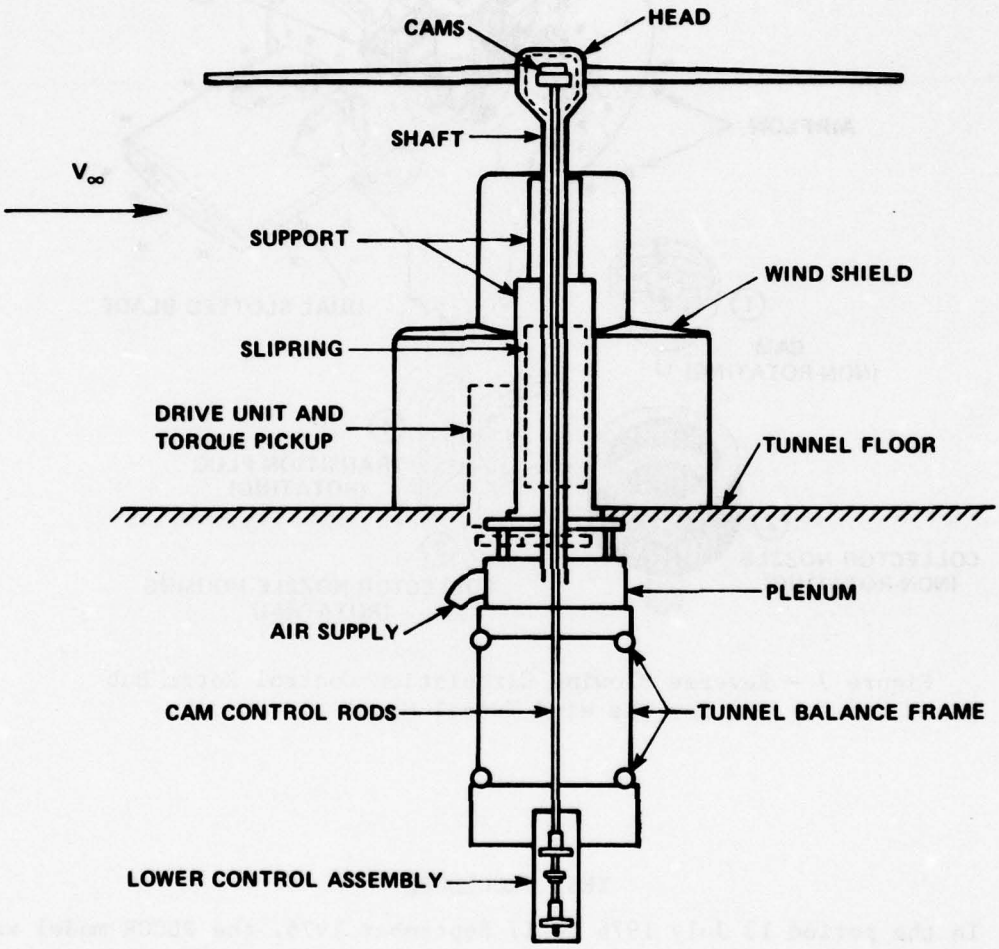

Figure 8 - Schematic of Circulation Control Rotor System in Wind Tunnel

control mechanism was attached to the balance frame. Tares due to the hydraulic and air supply lines were removed from the measured forces and moments.

With the addition of blade pressure to blade collective pitch angle as a variable for controlling rotor lift, a very extensive tunnel test program was required to determine near optimum flight conditions. After the shaft angle was set (positive shaft angle is rearward tilt), blade collective angles were set manually at the head. These angles were varied for -6 to 0 deg in the tunnel.

The rotor tip speed was then set at 100 or 250 ft/sec (30.5 or 76.2 m/s). After the rotor speed was set, the tunnel speed was set for a prescribed advance ratio. Tunnel temperature, humidity, and barometric pressure were monitored to maintain a constant tunnel velocity and the rotor speed was held constant while the rotor thrust-coefficient range was varied from 0.006 to 0.038 by varying supply pressure to the blade Coanda nozzles.

The control system provided the cyclic blowing that is required to trim the rotor in flight. Trimmed flight was assured by isolating rotor pitch and roll moments through the use of blade root flapping moments, a sine-cosine resolver, and an analog computer (see Figure 9).

Both dynamic and steady data were recorded for each test point. Time-dependent data were recorded on an oscillograph and steady state data were recorded from the six-component balance. (The rotor was also tested on a hover test stand at DTNSRDC, where a similar procedure was used.)

FORWARD FLIGHT RESULTS

Basic forward flight performance of the RBCCR model was obtained over a thrust range for different advance ratios, blade collective pitch angles, rotor tip speeds, and shaft angles. This report presents performance comparison at shaft angles of -5 to +2.5 deg at an advance ratio of 0.7. The effects of blade collective pitch angle, tip speed, and rotor thrust are presented at selected shaft angles.

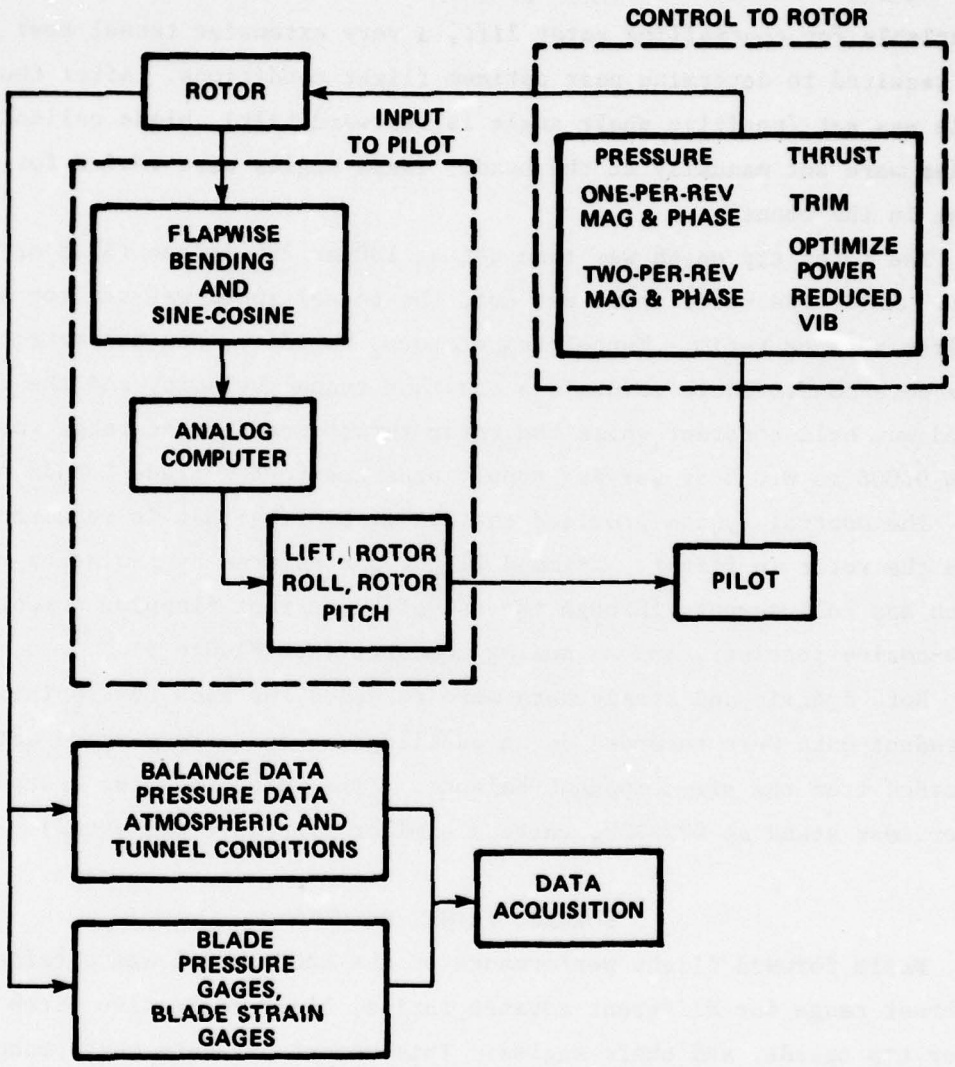

Figure 9 - Circulation Control Rotor Instrumentation and Control Schematic

SHAFT ANGLE EFFECTS

Experiments were conducted to determine the effects of rotor shaft angle on the performance of the RBCCR model in transition ($\mu = 0.7$). Typical shaft angle results are presented in Figures 10 through 15 for a blade collective angle of -4 deg and a hover tip Mach number of 0.22. The same basic 2P pressure wave (provided by cam number two) was used throughout this investigation.

Figure 10 shows the change in rotor total power and compressor power coefficient for shaft angles of -5 to +2.5 deg as thrust is increased. For a constant blade collective angle, both the total and compressor power is reduced with more positive shaft angles. The difference between the total power and compressor power curves is the rotor shaft power, and is given in Figure 11. A substantial reduction is noted in both compressor power and shaft power as shaft angle is increased. This reduction in power is reflected in an increase in rotor efficiency L/D_e as shaft angle is increased (Figure 12).

The lower thrust limit of the curve in Figures 10 through 15 is due to the minimum trim capabilities of the rotor; the upper thrust limit is due to model vibration and/or model trimmability. (A comparison of shaft angle effect for a constant effective collective blade angle (with respect to freestream) on the advancing side of the rotor shows about the same results presented in Figure 12. The effect of matching advancing tip blade angle on rotor efficiency will be discussed in the Rotor Thrust Augmentation Section.)

When the shaft angle is varied from zero, the frontal area of the rotor increases and reflects an increase in rotor drag. Figure 13 shows a typical variation in rotor C_D/σ versus C_L/σ for the range of shaft angles tested. These values of drag are included in the L/D_e curves presented in this report.

ROTOR THRUST AUGMENTATION

A measure of how well the RBCCR airfoils generate thrust can be seen by examining the rotor thrust augmentation. This analysis is analogous to

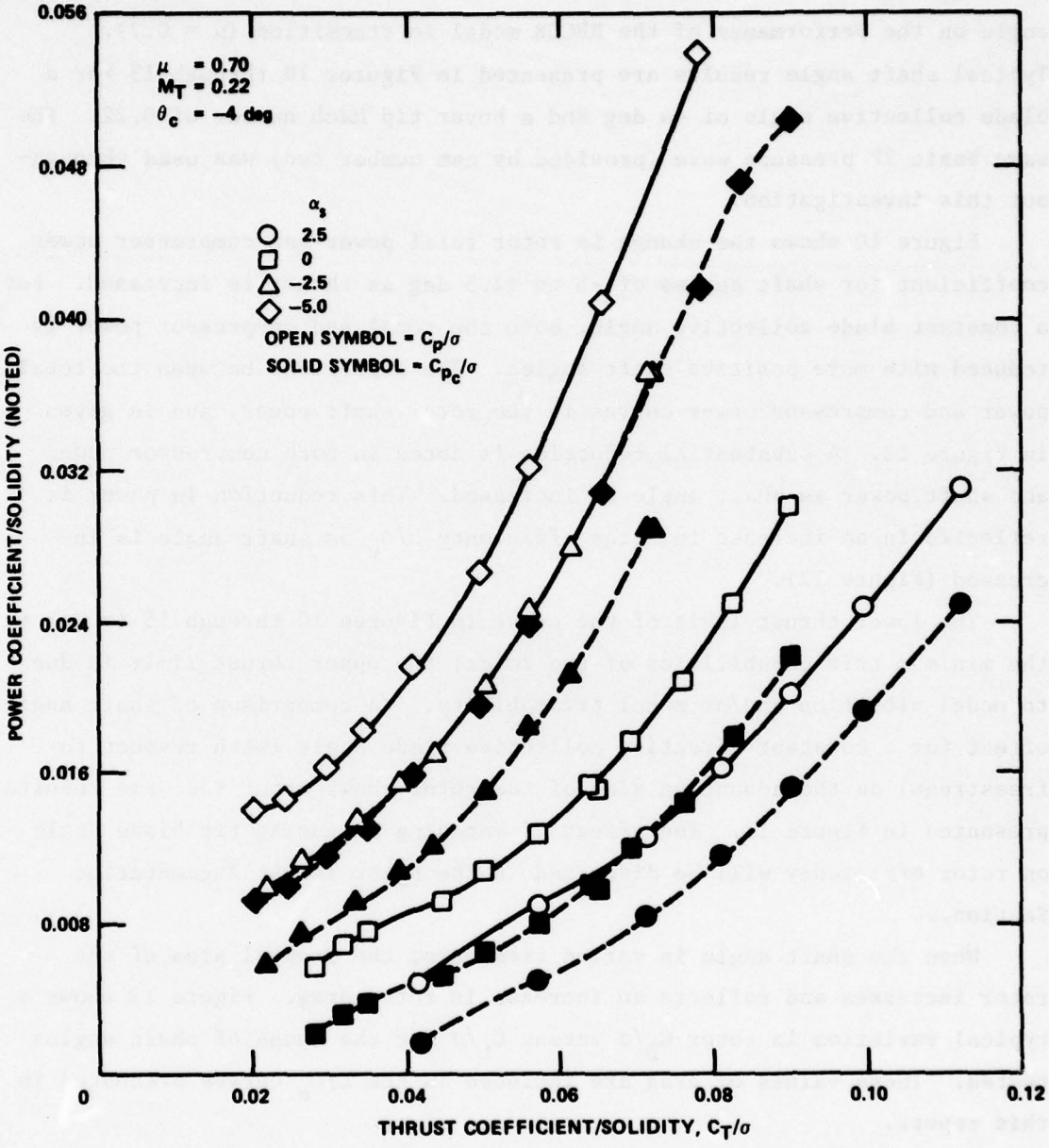

Figure 10 - Rotor Total and Compressor Power Variation with Thrust at Various Shaft Angles

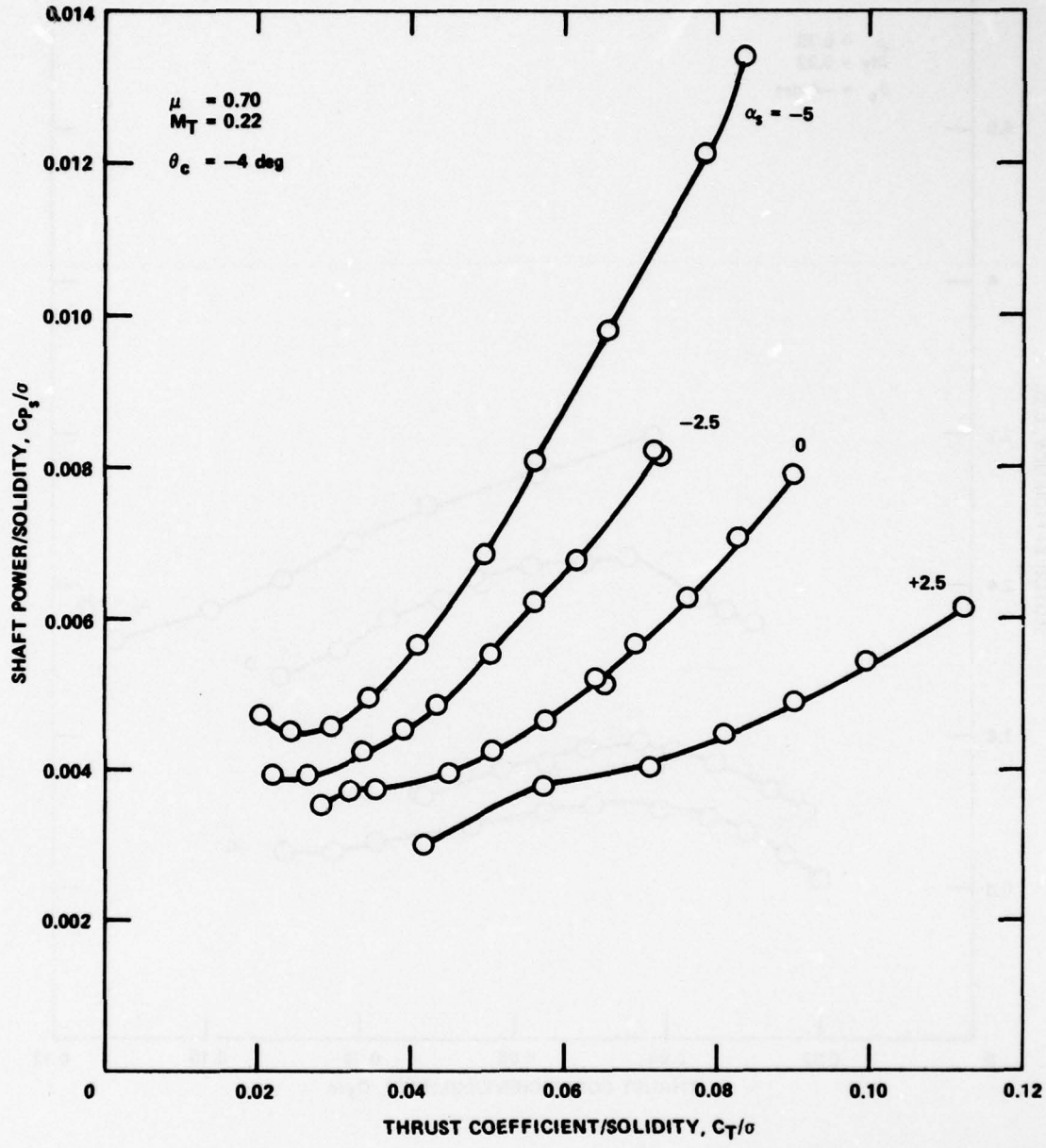

Figure 11 - Shaft Power Variation with Thrust at Various Shaft Angles

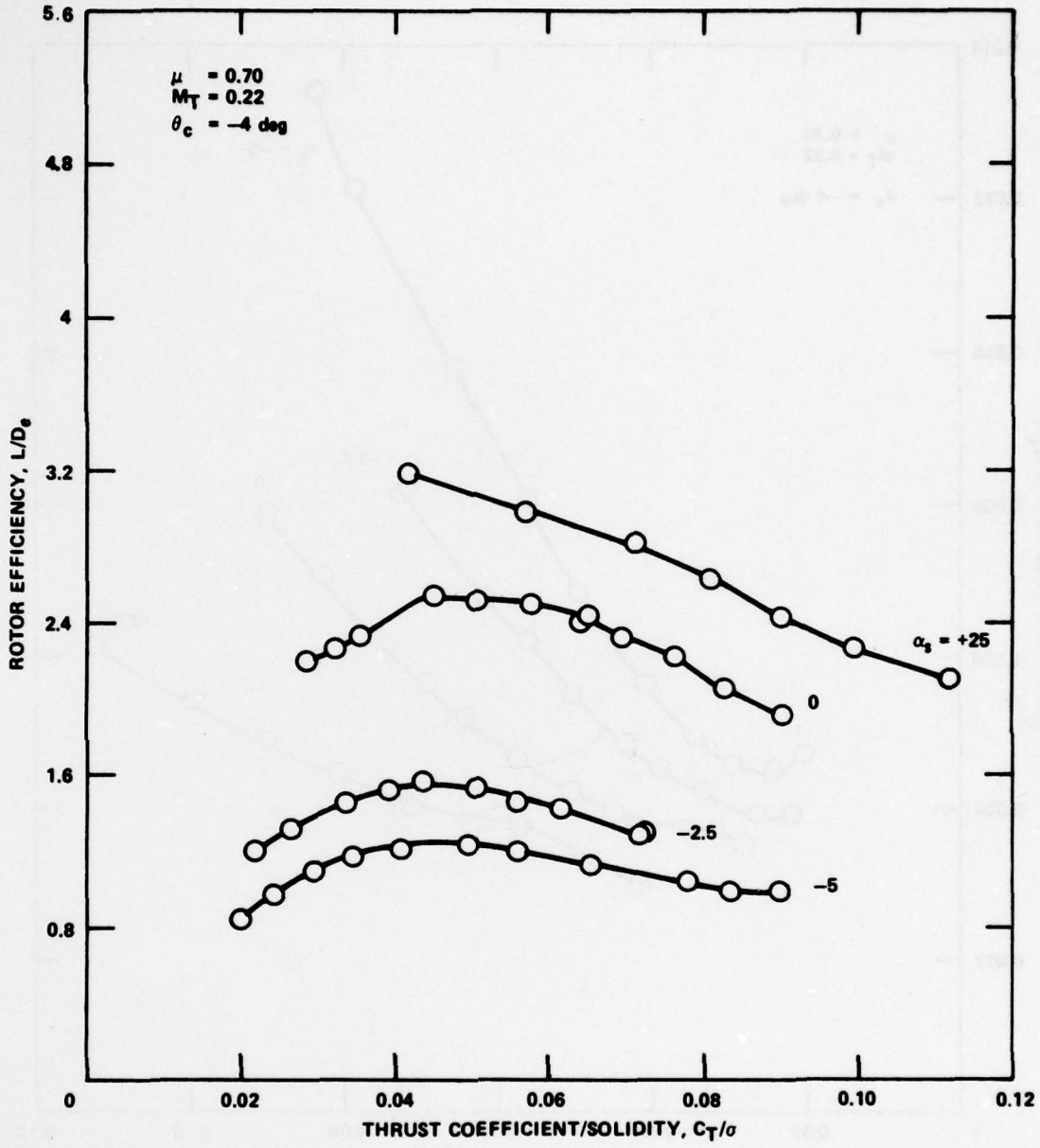

Figure 12 - Rotor Efficiency Variation with Thrust at Various Shaft Angles

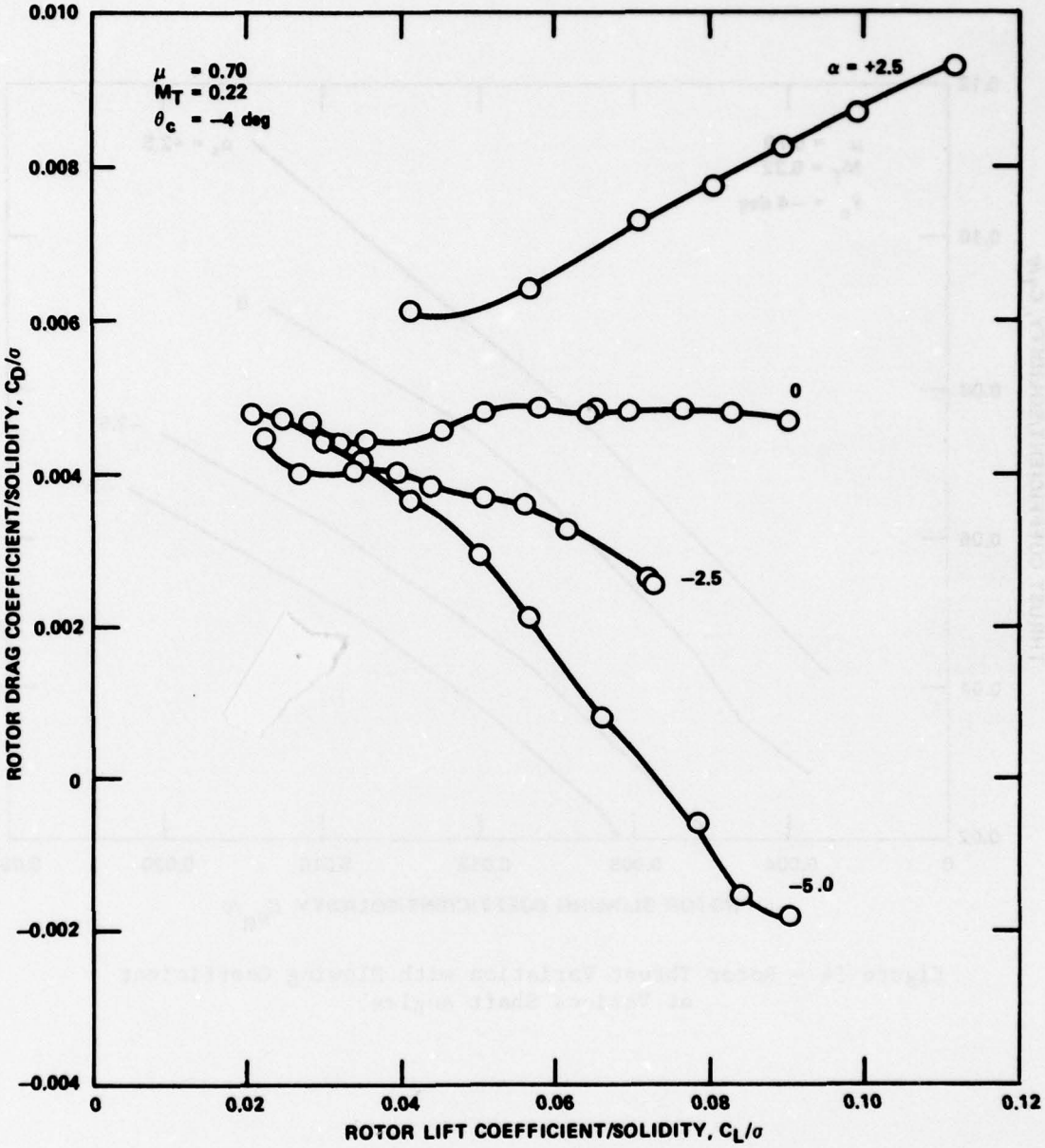

Figure 13 - Rotor Drag Variation with Lift at Various Shaft Angles

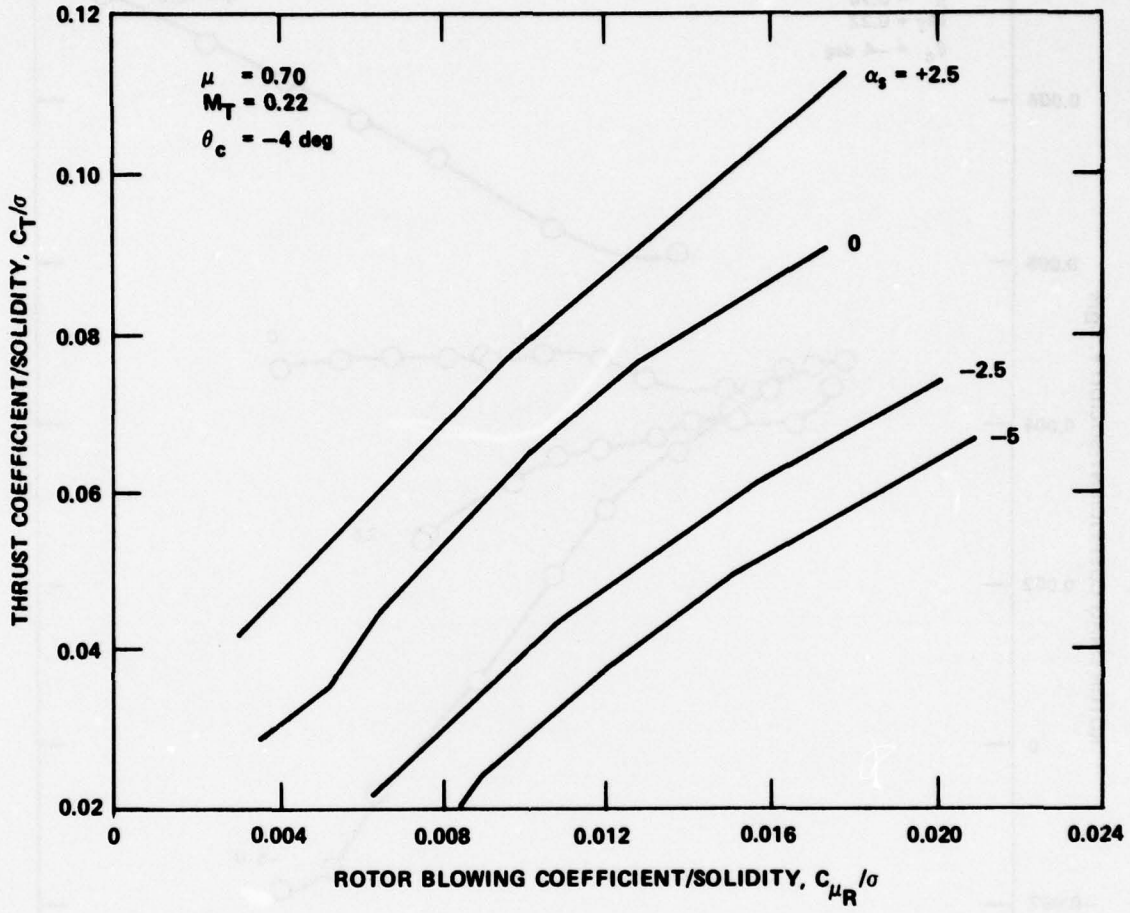

Figure 14 - Rotor Thrust Variation with Blowing Coefficient at Various Shaft Angles

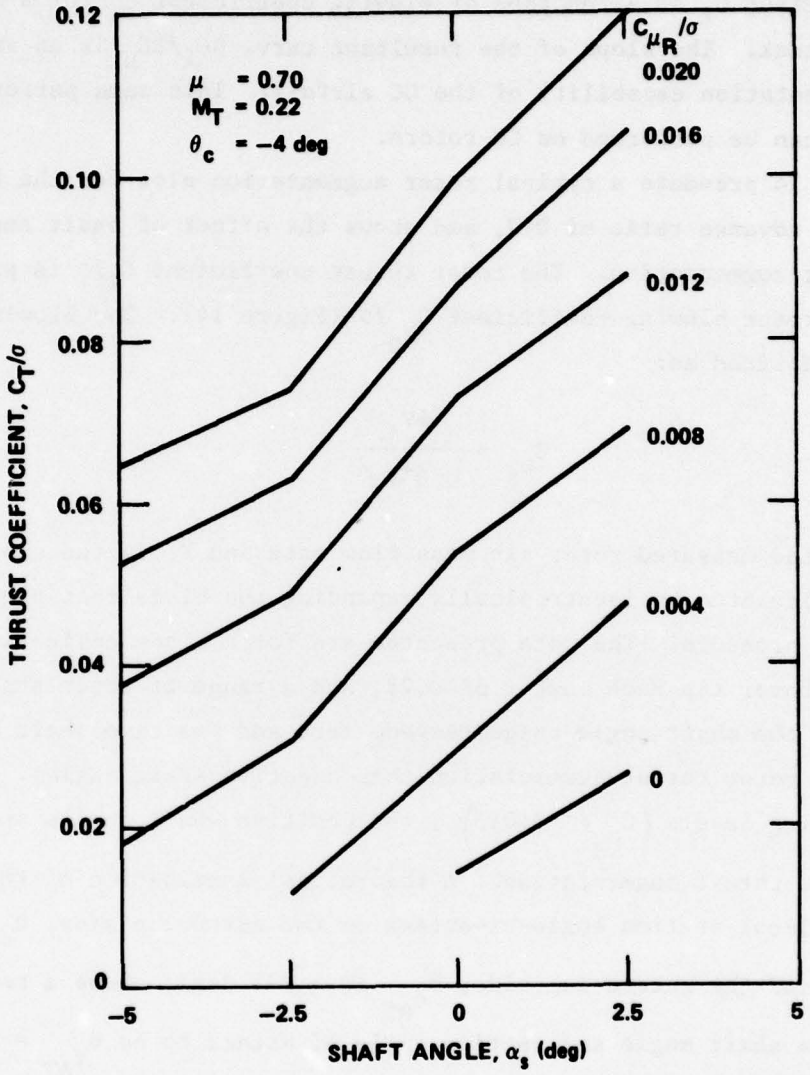

Figure 15 - Rotor Thrust Variation with Shaft Angle at Various Blowing Coefficients

the lift augmentation data that has been presented for two-dimensional investigation of CC airfoils.[10] The lift augmentation is obtained by plotting lift coefficient C_ℓ as a function of blowing coefficient C_μ for a constant angle of attack. The slope of the resultant curve $\Delta C_\ell / \Delta C_\mu$ is an indication of the augmentation capability of the CC airfoil. This same performance evaluation can be performed on CC rotors.

Figure 14 presents a typical rotor augmentation plot for the RBCCR model at an advance ratio of 0.7, and shows the effect of shaft angle on rotor thrust augmentation. The rotor thrust coefficient C_T/σ is plotted versus the rotor blowing coefficient C_{μ_R}/σ (Figure 14). The blowing coefficient is defined as:

$$C_{\mu_R} = \frac{\dot{m} V_j}{\rho \pi R^2 V_T^2}$$

where $\dot{m}$ is the measured rotor air mass flow rate and V_j is the slot jet velocity calculated by isentropically expanding the blade root pressure to atmospheric pressure. The data presented are for a blade collective angle of -4 deg, hover tip Mach number of 0.22, and a range of rotor shaft angles.

Within the shaft angle range tested, zero and positive shaft angles show better rotor thrust augmentation than negative shaft angles. At the higher blowing levels $\left(C_{\mu_R}/\sigma > 0.013\right)$, the positive shaft angles show improved rotor thrust augmentation. A theoretical examination of the rotor-blade-tip, local-section angle-of-attack on the advancing side, $\theta_{c_{AT}}$ at (ψ = 90 deg), and the retreating side, $\theta_{c_{RT}}$ (ψ = 270 deg), shows a relationship between shaft angle and section angle of attack to be $\theta_{c_{AT}} = 0.412\ \alpha_s - 4.03$ and $\theta_{c_{RT}} = 2.28\ \alpha_s - 4.16$, respectively. On the advancing side of the rotor, each 2.5-deg change in shaft angle increases the local angle of attack by 1.03 deg, whereas on the retreating side this increase is 5.70 deg. For shaft angles within the range of this study, the local-section angle-of-attack at the tip on the fore and aft portions of the disc are nearly the same as the local-section angle-of-attack of the advancing side.

Even though a majority of the lift is carried on the longitudinal portions of the rotor disc, the majority of rotor trim is produced on the lateral portions of the disc. The local-section angle-of-attack of the rotor blades for positive shaft angles is more conducive to good thrust augmentation (Figure 14), which is realized by an extended trim range and better rotor performance.

A typical crossplot of rotor thrust coefficient versus shaft angle for several constant blowing coefficients is presented in Figure 15. A substantial increase in the thrust-coefficient-to-shaft-angle slope is noted for shaft angles greater than -2.5 deg.

ROTOR BLADE COLLECTIVE PITCH ANGLE

Experiments were conducted to determine the effect of rotor blade collective pitch angle on rotor thrust, efficiency, and power. Typical relationships between blade collective angle and rotor thrust for constant values of blowing coefficient are presented in Figures 16a and 16b. These respective plots are for the extremities of the shaft angle range tested; +2.5 and -5.0 deg.

Due to the interaction of blade collective angle and shaft angle, as discussed earlier, the maximum blade collective for a given shaft angle is limited by the rotor becoming untrimmable (excessive lift on the advancing side due to angle-of-attack). The forward flight performance program (CRUISE 4) established the trim-limit blade collective angle as a function of shaft angle. This relationship, $\theta_c = -0.6647\ \alpha_s - 0.7$, establishes the maximum blade collective angle at each shaft angle for which the rotor can be trimmed. Good agreement was obtained between the rotor model trim limit and this equation (see Figure 17).

The trend of rotor efficiency (L/D_e) with blade collective angle and rotor shaft angle at a constant $C_T/\sigma = 0.06$ is presented in Figure 18 for a transitional advance ratio of 0.7. In general, as blade collective angle and rotor shaft angle are increased, rotor efficiency increases until a trim limit is reached (established by Figure 17). A subtlety that should

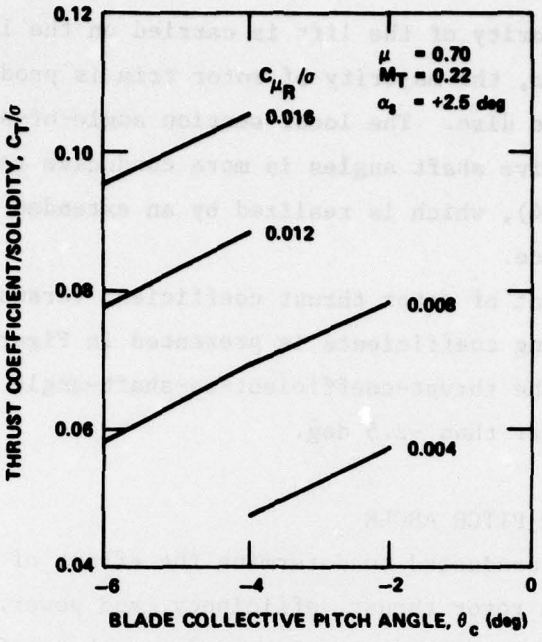

Figure 16a - Shaft Angle +2.5 Degrees

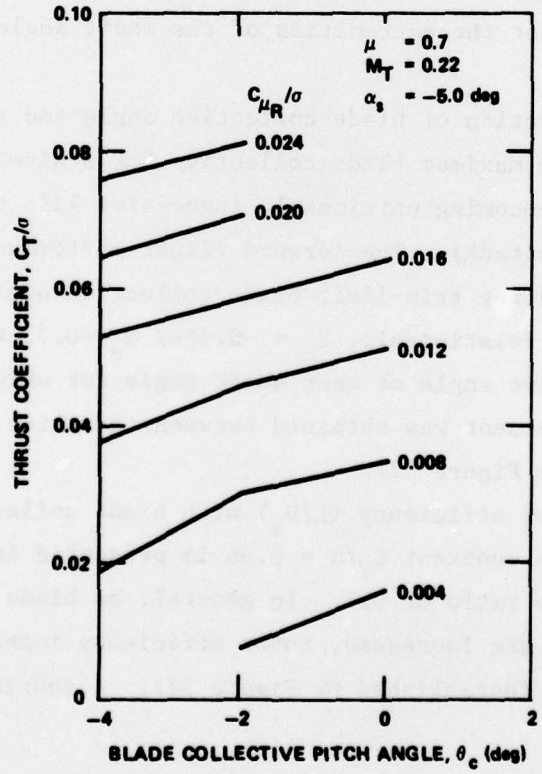

Figure 16b - Shaft Angle -5.0 Degrees

Figure 16 - Rotor Thrust Variation with Blade Collective Pitch Angle at Various Blowing Coefficients

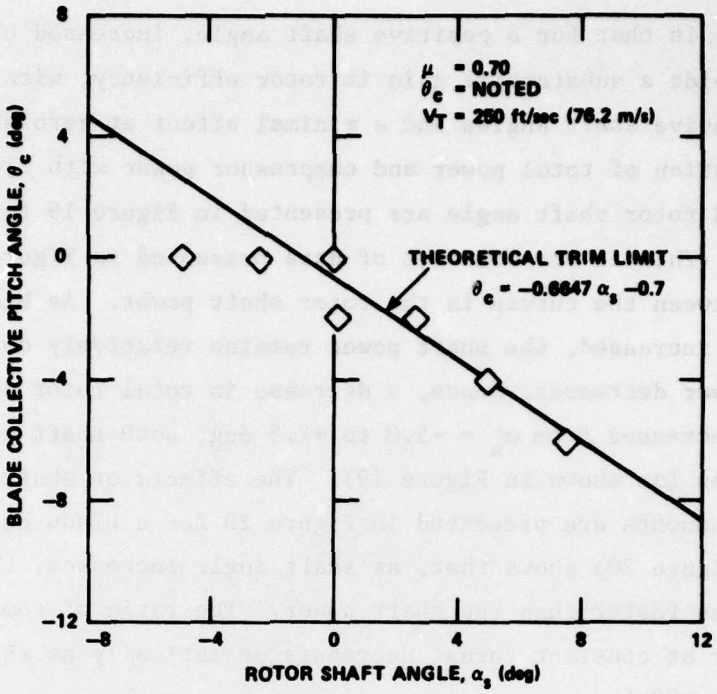

Figure 17 - Rotor Shaft Angle--Blade Collective Pitch Angle Trim Limit

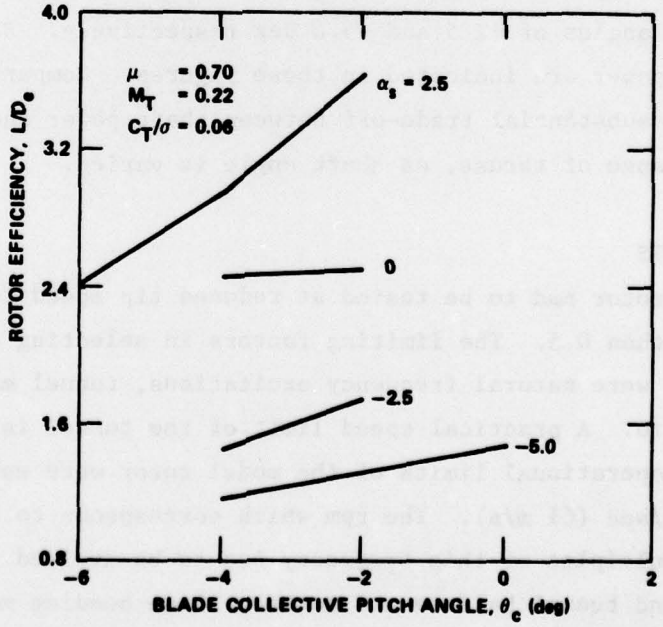

Figure 18 - Rotor Efficiency Variation with Blade Collective Pitch Angle at Several Shaft Angles

be pointed out is that for a positive shaft angle, increased blade collective angle yields a substantial gain in rotor efficiency, with a reduced effect at negative shaft angles and a minimal effect at zero shaft angle.

The variation of total power and compressor power with blade collective angle and rotor shaft angle are presented in Figure 19 for a constant $C_T/\sigma = 0.06$. (This is the same set of data presented in Figure 18.) The difference between the curves is the rotor shaft power. As blade collective angle is increased, the shaft power remains relatively constant and compressor power decreases; hence, a decrease in total rotor power. As shaft angle increases from $\alpha_s = -5.0$ to +2.5 deg, both shaft and compressor power decreases (as shown in Figure 19). The effects of shaft angle on the power components are presented in Figure 20 for a blade collective angle of -2 deg. Figure 20a shows that, as shaft angle increases, the compressor power decreases faster than the shaft power. The ratio of compressor power to shaft power at constant thrust decreases dramatically as shaft angle increases (Figure 20b).

Typical trends of shaft power and compressor power with thrust are examined at the extremities of the shaft angle range tested. These data are presented in Figures 21a and 21b as the compressor-power-to-total-power ratio for shaft angles of +2.5 and -5.0 deg respectively. Both shaft power and compressor power are indicated in these figures. Comparison of the figures shows a substantial trade-off between shaft power and compressor power, over a range of thrust, as shaft angle is varied.

TIP SPEED EFFECTS

The model rotor had to be tested at reduced tip speed for advance ratios greater than 0.5. The limiting factors in selecting a tip speed for the model rotor were natural frequency excitations, tunnel maximum speed, and advance ratio. A practical speed limit of the tunnel is 200 ft/sec (61 m/s). The operational limits of the model rotor were established by $\mu \times V_T \leq 200$ ft/sec (61 m/s). The rpm which corresponds to blade natural frequency and multiples of this frequency had to be avoided to keep from exciting the wind tunnel balance and to keep blade bending moments within structural limits.

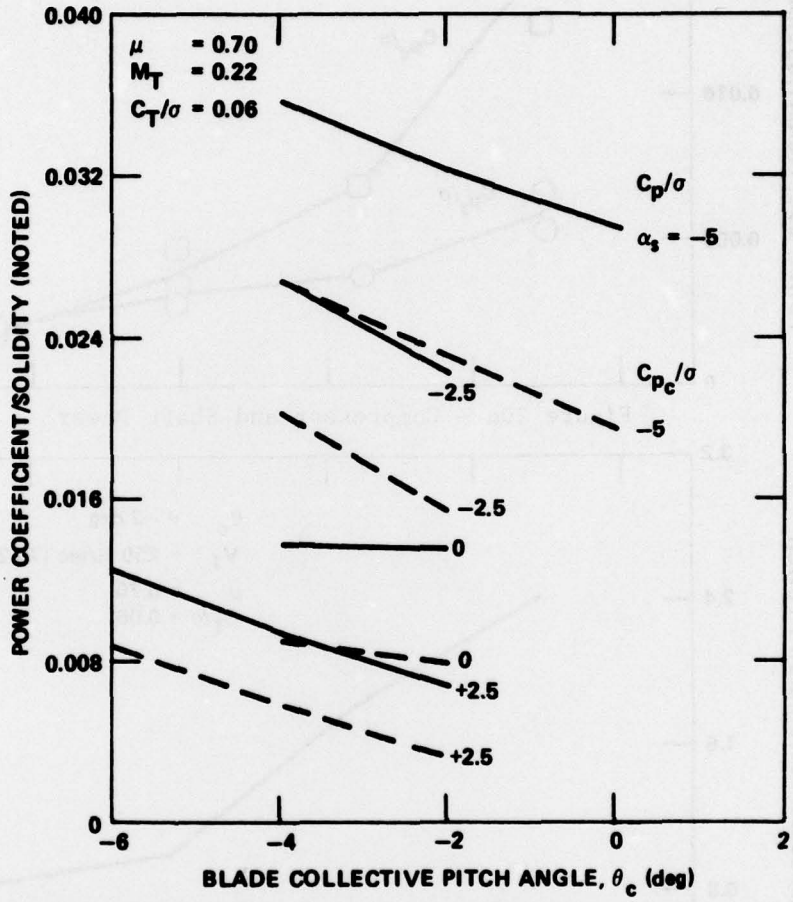

Figure 19 - Rotor Total and Compressor Power Variation with Blade Collective Pitch Angle at Several Shaft Angles

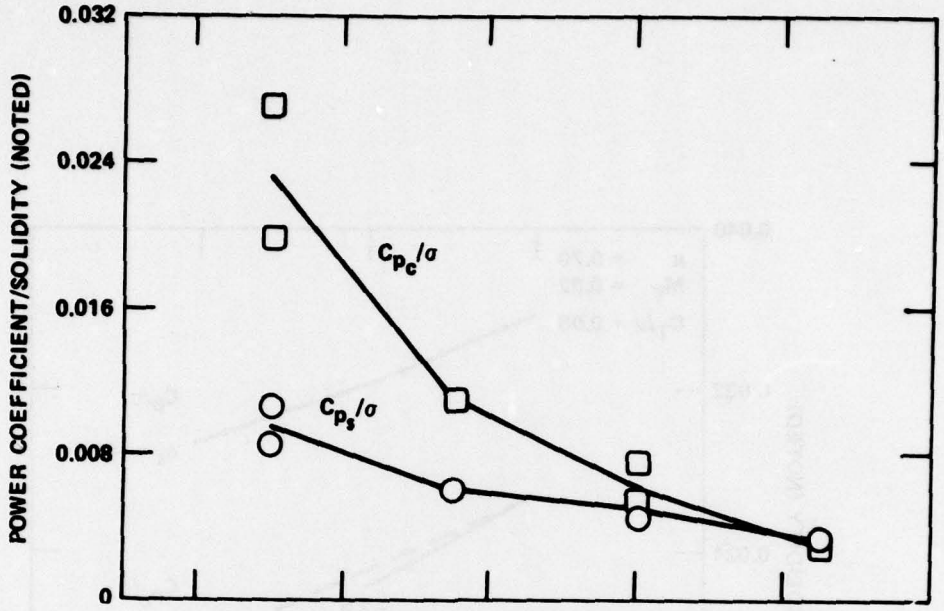

Figure 20a - Compressor and Shaft Power

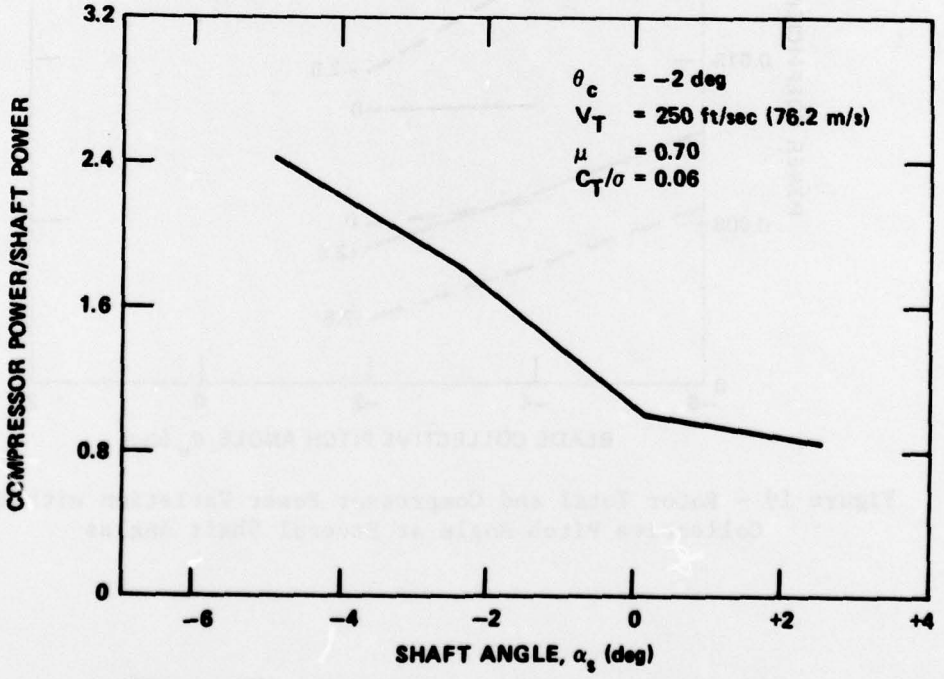

Figure 20b - Compressor-to-Shaft-Power Ratio

Figure 20 - Rotor Power Component Variation with Shaft Angles

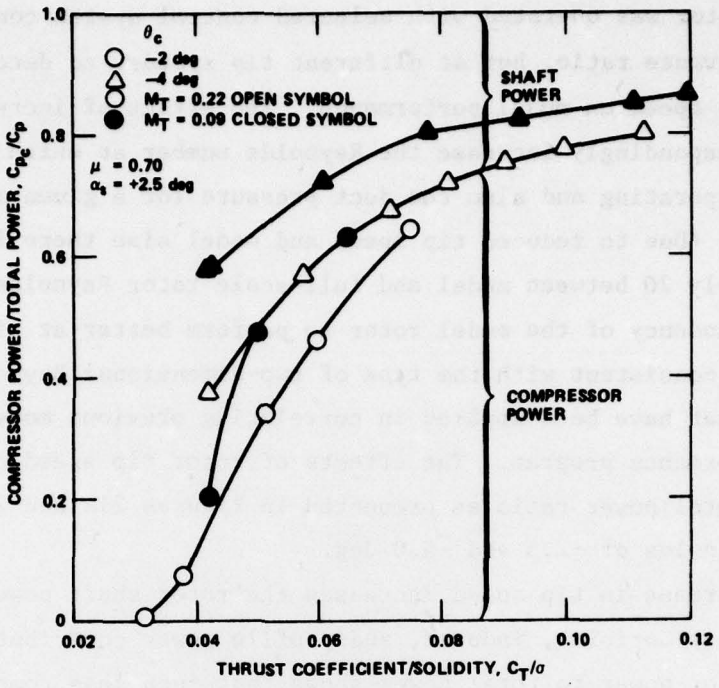

Figure 21a - Shaft Angle +2.5 Degrees

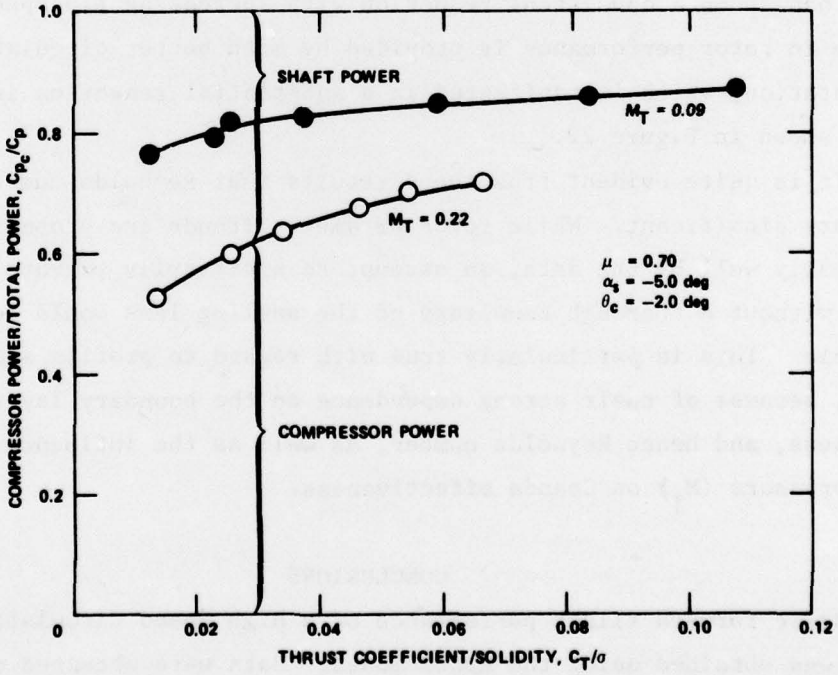

Figure 21b - Shaft Angle -5.0 Degrees

Figure 21 - Rotor Compressor Power Ratio Variation with Thrust

The rotor was operated with selected control system configurations for the same advance ratio, but at different tip speeds, to determine the effect of tip speed on model performance. The effect of increasing tip speed is to correspondingly increase the Reynolds number at which the blade sections are operating and also the duct pressure for a given momentum coefficient. (Due to reduced tip speed and model size there is a factor of approximately 20 between model and full-scale rotor Reynolds number.)

The tendency of the model rotor to perform better at higher Reynolds numbers is consistent with the type of two-dimensional Reynolds number corrections that have been applied in correlating previous model rotors to the rotor performance program. The effects of rotor tip speed on compressor power to total power ratio as presented in Figures 21a and 21b respectively for shaft angles of +2.5 and -5.0 deg.

An increase in tip speed increases the rotor shaft power whose magnitude reflects Coriolis, induced, and profile power contributions. The ratio of compressor power to total power shows that much less compressor power is required at the high tip speed. The ratio of compressor power to total power has shown a consistent reduction with increasing tip speed. The increase in rotor performance is provided by much better circulation control augmentation, which is manifested in a substantial reduction in compressor power shown in Figure 22.

It is quite evident from these results that Reynolds number effects are very significant. While rotor parameter trends are probably represented reasonably well by the data, an attempt to arbitrarily extrapolate to full-scale without a thorough knowledge of the scaling laws would be very questionable. This is particularly true with regard to profile and compressor power, because of their strong dependence on the boundary layer momentum thickness, and hence Reynolds number, as well as the influence of increased duct pressure (M_j) on Coanda effectiveness.

CONCLUSIONS

Basic forward flight performance of a High Speed Circulation Control Rotor was obtained using the RBCCR model. Data were obtained over a thrust

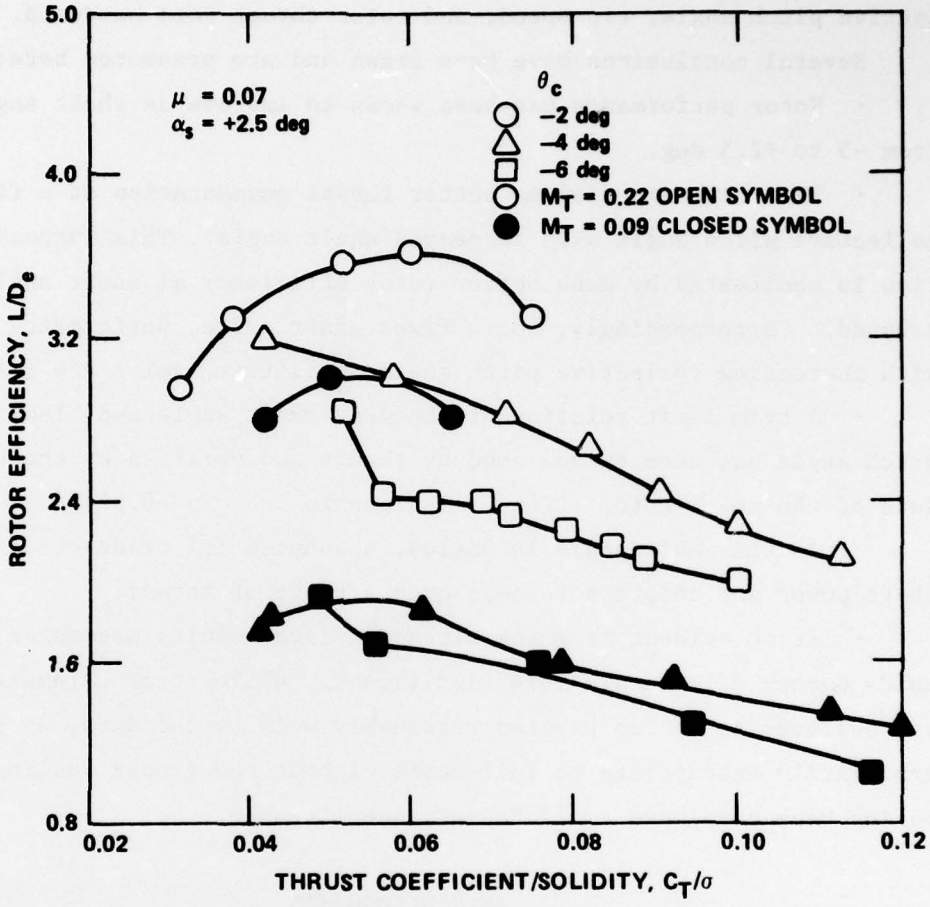

Figure 22 - Rotor Efficiency Variation with Thrust for Two Tip Speeds

range for different advance ratios, blade collective pitch angles, rotor tip speeds, and shaft angles. This report presents the most significant findings and trade-offs for a shaft angle range of -5 to +2.5 deg at an advance ratio of 0.7. At selected shaft angles, the effects of blade collective pitch angle, tip speed, and rotor thrust were assessed.

Several conclusions have been drawn and are presented here:

- Rotor performance has been shown to improve as shaft angle increases from -5 to +2.5 deg.
- The rotor experiences better thrust augmentation at a fixed blade collective pitch angle with increased shaft angle. This increased augmentation is manifested by much better rotor efficiency as shaft angle is increased. Correspondingly, for a fixed shaft angle, performance improves with increasing collective pitch angle until trim limits are reached.
- A trim limit relationship between shaft angle and blade collective pitch angle has been established by theory and verified by the wind tunnel data of the model rotor. This relationship is $\theta_c = -0.6647\ \alpha_s - 0.7$.
- As the shaft angle is varied, a substantial trade-off exists between shaft power and compressor power over a range of thrust.
- It is evident from the tip-speed data results presented that Reynolds number effects are very significant. While rotor parameter trends are believed to be represented reasonably well by the data, an attempt to arbitrarily extrapolate to full-scale without the proper scaling laws having been developed would be very questionable.

ACKNOWLEDGMENTS

The author would like to recognize the significant contribution of Mr. Gary Smith for assistance in conducting the experiments and reducing the data, and Mr. Martin Cook for his assistance in conducting the experiments.

REFERENCES

1. Reader, K.R. and J.B. Wilkerson, "Circulation Control Applied to a High Speed Helicopter Rotor," Paper 1003, 32nd National Annual Forum of the American Helicopter Society, Washington, D.C. (May 1976).

2. Smith, M.C.G., "The Aerodynamic of a Circulation Controlled Rotor," 3rd CAL/AVLABS Symposium On Aerodynamics of Rotary Wing Aircraft, Buffalo, N.Y. (Jun 1969).

3. Williams, R.M. and E.O. Rogers, "Design Considerations of Circulation Control Rotors," Paper 603, 28th National Annual Forum of the American Helicopter Society, Washington, D.C. (May 1972).

4. Wilkerson, J.B., "Design and Performance Analysis of A Prototype Circulation Control Rotor," NSRDC ASED AL-290 (Mar 1973).

5. Wilkerson, J.B. and D.W. Linck, "A Model Rotor Validation for the CCR Technology Demonstrator," Paper 902, 31st National Annual Forum of the American Helicopter Society, Washington, D.C. (May 1975).

6. "Design Study of A Flight Worthy Circulation Control Rotor System," Kaman Aerospace Corporation Report R-1036-2, Contract N00019-73-C-0429 (Jul 1974).

7. "Design Study of A Helicopter with A Circulation Control Rotor (CCR)," Lockheed Report LR26417, Contract N00019-73-C-0435 (May 1974).

8. Williams, R.M., "Application of Circulation Control Rotor Technology to A Stopped Rotor Aircraft Design," First European Rotorcraft and Powered Lift Aircraft Forum, Southampton, England (22-23 Sep 1976).

9. Reader, K.R., "Control System for A Reverse Blowing Circulation Control Rotor (RBCCR) Wind Tunnel Model," NSRDC Report 76-0062 (May 1976).

10. Stone, M.B. and R.J. Englar, "Circulation Control - A Bibliography of NSRDC Research and Selected Outside References," NSRDC Report 4108 (Jan 1974).

INITIAL DISTRIBUTION

Copies	
1	ARO/Engr Sci Div S. Kumar, Asso Dir
1	AASC/Lib
1	AAMCA/AMXAM-SM
2	AAMRDL/Ft. Eustis 1 Lib 1 SAVRE-AM
2	AAMRDL/Ames Res Cen 1 Tech Dir 1 A. Kerr
1	CMC/Sci Advisor A.L. Slafkosky
1	ONR/Aeronautics, Code 461
2	NRL 1 Tech Info Office 1 Lib, Code 2029
1	USNA
2	NAVPSCOL 1 J. Miller 1 L. Schmidt
4	NAVAIRDEVCEN 1 Tech Dir 1 Tech Lib 1 R. McGiboney 1 G. Woods
15	NAVAIRSYSCOM 1 AIR 03 1 AIR 03A (F. Tanczos) 1 AIR 03PA (H. Andrews) 1 AIR 03P (Capt Miller) 2 AIR 320D (D. Kirkpatrick) 1 AIR 320B (G. Unger) 1 AIR 5104 1 AIR 530B 1 AIR 5301 (F. Paglianete) 1 AIR 530214A 1 AIR 530112

Copies	
	NAVAIRSYSCOM (Continued) 1 AIR 530122 (R. Tracey) 1 AIR 604 1 AIR PMA-247
3	NAVAIRTESTCEN 1 Dir, TPS 1 N. Jubeck 1 Rotary Wing Directorate
12	DTIC
1	AF Dep Chief of Staff AFRDT-EX
2	AFFDL 1 FDV, VTOL Tech Div 1 FDMM, Aeromech Br
1	AFOSR/Mechanics Div
1	FAA, Code DS-22 V/STOL Programs
3	NASA HQ 1 A. Evans 1 A. Gessow 1 J. Ward (MS-85)
6	NASA Ames Res Cen 1 Tech Lib 1 Full-Scale Res Div 1 M. Kelley/Lg-Scale Aero Br 1 J. McCloud 1 J. Rabbot 1 J. Biggers
3	NASA Langley Res Cen 1 Tech Lib 1 R. Tapscott 1 G. Hammond
2	West Va U/Dept Aero Engr 1 J. Fannuci 1 J. Loth

Copies	
1	Analytical Methods/F. Dvorak
1	Bell Aerospace Corp/Ft. Worth/Lib
2	Boeing Co/Seattle 1 Tech Lib 1 P.E. Ruppert
2	Boeing Co/Vertol Div 1 Tech Lib 1 B. Walls
1	Fairchild-Hiller/Farmingdale 1 Republic Aviation Div
1	Gen Dyn/Convair Div Tech Lib
1	Grumman Aerospace Corp M. Siegel
2	Honeywell, Inc/S&R Div 1 Tech Lib
3	Hughes Tool Co/Culver City 1 E. Wood 1 A/C Div 1 A. Logan
3	Kaman Aerospace Corp 1 Tech Lib 1 D. Barnes 1 A. Lemnios
1	Ling-Temco-Vought, Inc/Lib
7	Lockheed A/C Corp/Burbank 1 Tech Lib 4 P. Kesling 1 B.R. Rich 1 B. Radoll
1	Lockheed-Georgia Corp/Lib
1	McDonnell-Douglas/Long Be T. Cebeci

Copies	
1	Northrop Corp/Hawthorne Lib
1	Paragon Pacific Inc. J.H. Hoffman
1	Rochester Appl Sci Asso, Inc/Lib
2	United A/C Corp/E. Hartford 1 Tech Lib 1 J. Landgrebe
3	United A/C Corp/Sikorsky 1 Lib 1 T. Carter 1 E. Fradenburgh

CENTER DISTRIBUTION

Copies	Code	Name
10	5211.1	Reports Distribution
1	522.1	Library (C)
1	522.2	Library (A)
2	522.3	Aerodynamics Lib